J-QE/23/10//16042

Ultrasensitive Time-Resolved Polarized Fluorescence Spectroscopy as a Tool in Biology and Medicine

A. Van Hoek
K. Vos
A.J.W.G. Visser

Reprinted from
IEEE JOURNAL OF QUANTUM ELECTRONICS
Vol. QE-23, No. 10, October 1987

Ultrasensitive Time-Resolved Polarized Fluorescence Spectroscopy as a Tool in Biology and Medicine

A. VAN HOEK, K. VOS AND A. J. W. G. VISSER

Abstract—**Fluorescence induced by mode-locked and synchronously pumped continuous wave lasers and detected by time-resolved single-photon counting is a sensitive and dynamic property to be utilized in a wide variety of biological and medical applications. Examples are given to illustrate the potency of the technique.**

INTRODUCTION

MOST biological systems produce fluorescence upon light excitation of intrinsic or externally inserted chromophores [1]–[3]. A specialized form of fluorescence technique, namely, time-resolved polarized fluorescence, provides information on properties like mobility and local environment and on processes like energy transfer, or it simply characterizes the fluorescent reporter group in complex biological structures.

When a sample is excited with a pulse of linearly polarized light, only those chromophores with absorption dipole moment in the plane of light polarization will be excited. An anisotropic excitation of chromophores or photoselection is then created. Fluorescence from these molecules will have a preferred polarization direction with respect to the absorption dipole moment. When excitation is within the lowest energetic absorption band, the fluorescence transition dipole moment is identical to that of absorption. Between the time of excitation and emission, i.e., during the fluorescence lifetime, several dynamic effects can influence the direction of fluorescence polarization, causing a decrease in fluorescence polarization or depolarization. For instance, the molecules can rotate, or alternatively, excitation energy is transferred to another chromophore, also affecting the polarization direction. Different examples of the first type are outlined in detail below.

Time-dependent fluorescence depolarization is commonly expressed in the so-called fluorescence anisotropy $r(t)$, which is defined as

$$r(t) = \frac{i_{/\!/}(t) - i_{\perp}(t)}{i_{/\!/}(t) + 2i_{\perp}(t)} \qquad (1)$$

where $i_{/\!/}(t)$ and $i_{\perp}(t)$ are the decays of fluorescence, polarized, respectively, parallel and perpendicular with respect to the polarization direction of the excitation light.

Manuscript received December 30, 1986; revised April 13, 1987.

The authors are with the Departments of Molecular Physics and Biochemistry, Agricultural University, De Dreijen 11, 6703 BC Wageningen, The Netherlands.

IEEE Log Number 8716042.

Powerful short-pulse laser sources are available for kinetic optical spectroscopy. Nevertheless, the high energies available cannot always be used for excitation because of the introduction of secondary effects like saturation, photolysis, and exciton annihilation in, for instance, photosynthetic pigments [4]. To be able to use low-energy laser pulses, the collection and detection of emitted fluorescence should be as efficient as possible. This is also important when measuring fluorescence from very diluted samples. Such dilution can be due to poor yield of isolation and purification or to experimental requirements (wide-range concentration series or preventing interaction of chromophores).

Time-resolved single-photon counting is the most efficient method to detect emission with a time resolution of some tens of picoseconds. With this technique, every emitted photon that can be collected by the optics and photomultiplier will be used as data. That is not the case with, for instance, optical gating techniques [6], which have superior time resolution, but degraded detection efficiency since only the fraction of photons within the gate out of all available emitted photons are used as data. Synchroscan streak cameras equipped with microchannel plate image intensifiers can detect emission at the single-photon level [7], at comparable detection efficiency and time resolution. Disadvantages are the high price of the camera system, the limited dynamic range, and the fact that noise in the data does not have a Poisson character. The Poisson character of noise in data from time-resolved single-photon counting can effectively be used in the fitting procedure. In addition, the high excitation rate to be used in synchroscan experiments can easily cause exciton annihilation in, for example, photosynthetic pigments [4].

EXPERIMENTAL METHODS

A block diagram of the experimental setup is given in Fig. 1. For excitation of the samples, a mode-locked CW argon ion laser [8], [9] or a synchronously pumped CW dye laser [10] was used, supplying pulses with nanojoule energies at a repetition rate of 76 MHz. From the ion laser, the argon lines ranging from 351 to 514 nm in wavelength were used [pulses about 100 ps full width at half maximum (FWHM)]. In the dye laser, Rhodamine 6G was used, lasing from 570 to 630 nm (pulses 5 ps FWHM). An ADA frequency-doubling crystal could be incorporated to obtain wavelengths from 290 to 310 nm [11]. In most experiments, an extra-cavity electrooptic modulator

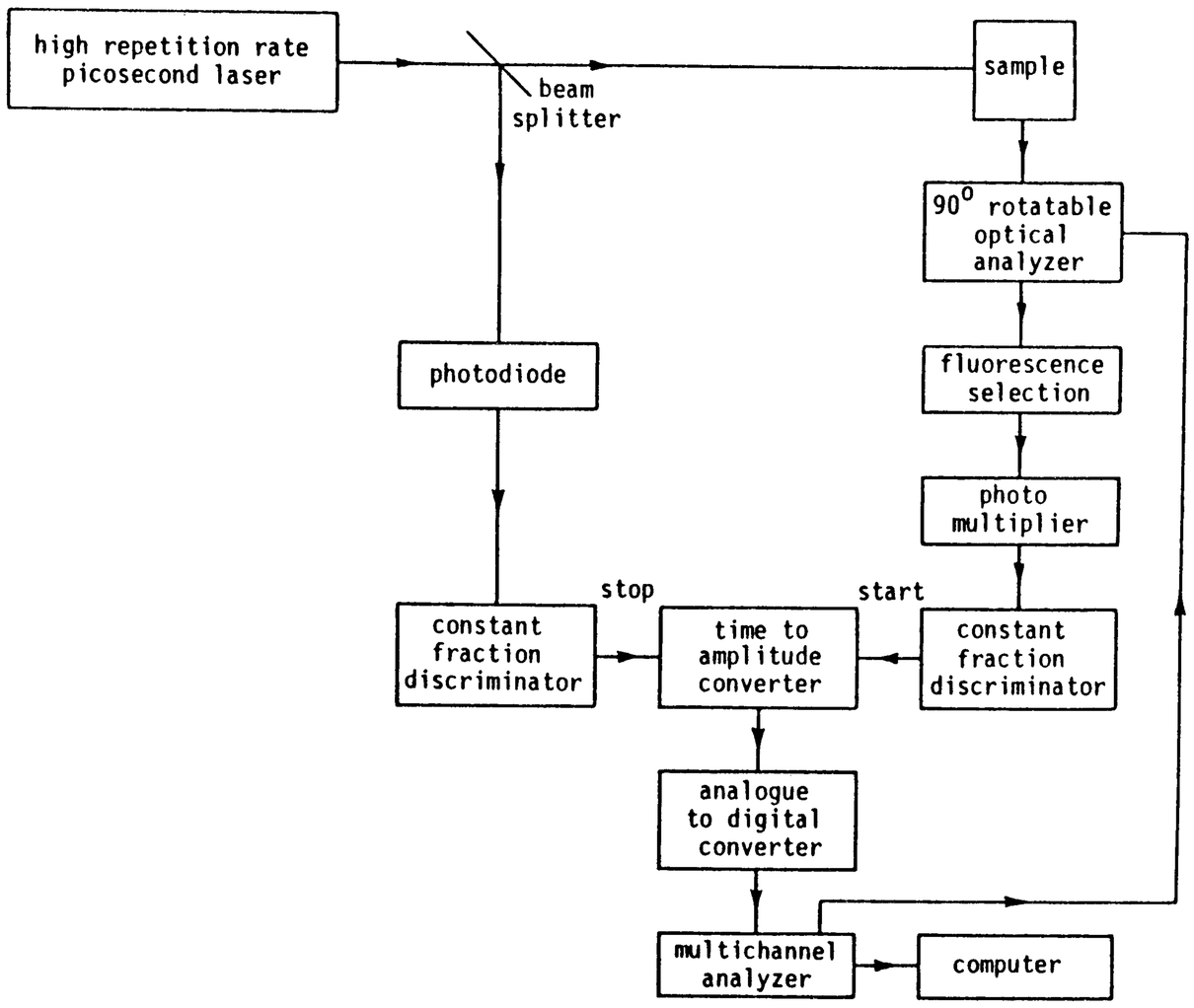

Fig. 1. Block diagram of the experimental setup.

setup was used [12] to decrease the repetition rate of excitation pulses to 600 kHz or any power of 2 lower.

The sample housing was able to contain both a liquid helium flow cryostat and a thermostatable cuvette holder for measurements at physiological temperatures. In the cuvettes an 0.2 mL sample was sufficient for the experiments at chromophore concentrations down to the nanomolar region.

Fluorescence emission was detected perpendicular to the direction of the exciting beam, through an interference filter and a sheet polarizer (Polaroid-type HNP'B for the UV and HN38 or NH22 for the visible region of the spectrum). An interference filter and a polarizer sheet were preferred over a monochromator and a prism polarizer because of their ability to collect fluorescence emission with simple high-throughput optics.

The polarizer sheet was mounted on a ball-bearing holder, driven by two computer-controlled rotation magnets to select emission polarized parallel or perpendicular to the polarization of the exciting beam. A 90° rotation of the holder took approximately 0.3 s. That should be a short period of time because the experiment consisted of many equal periods of measuring parallel and perpendicular polarized fluorescence components, between which the polarizer was rotated every time. In that way, the long-term fluctuations of excitation power were averaged out. In practice, the experiment consisted of 2×10 periods of collecting data from parallel and perpendicular polarized fluorescence, all of which lasted 10 s.

In time-corelated single-photon counting [13], fluorescence photons were detected by a photomultiplier, supplying a pulse at the anode as a response to one photon impact at the cathode. These pulses were normalized using a constant fraction discriminator, and with a time-to-amplitude converter, the time span between an exciting light pulse and a fluorescence photon was converted to an analog pulse height. Therefore, only one photon per excitation pulse could be detected.

The analog pulse heights were analyzed by an ADC, and these data were collected in a multichannel analyzer. In this way, a decay was built up from a large number of photon events, using the statistical distribution in time of fluorescence photons referred to the excitation moment. The time resolution of the setup was mainly limited by transit-time jitter in the photomultiplier [5], a Philips PM 2254 B. This resulted in a pulsewidth of the overall temporal response of about 500 ps FWHM, depending somewhat on the wavelength of detection. Next to that, an afterpulse was apparent in the data (see, for instance, Fig. 4(a), curve b) at about 14 ns after the main peak, which is due to scattering of electrons in the first dynode region of the photomultiplier [5]. Data from the multichannel analyzer were transferred to a Micro-VAX II computer for data analysis.

Data Analysis

During data analysis, requirements often come through about experimental conditions. In this case, where a deconvolution procedure was used to be able to recover short decay times with sufficient accuracy [14], next to a fast dynamic response of the apparatus, the absence of temporal shifts of the timing signals was essential to attain reproducibility [15]. Therefore, a stable ambient temperature during the experiments and an extensive equilibration of the setup was important, and last but not least, the reference experiments for the deconvolution procedure had to be recorded with the apparatus in the same configuration as during the measurement of the sample to be investigated [16].

For that purpose, a reference compound was used [17] with short and single-exponential fluorescence decay and absorbance and emission in the same wavelength region

as the unknown sample. In practice, every experimental recording was flanked in time by two recordings of the reference compound, and data of these references were averaged.

A detailed description of our methods for data analysis is given in [18]. In this section, we will restrict ourselves to models where both the fluorescence $s(t)$ and the anisotropy $r(t)$ have (the sum of) exponential decays:

$$s(t) = i_{/\!/}(t) + 2i_{\perp}(t) = \sum_i \alpha_i \exp(-t/\tau_i) \quad (2)$$

$$r(t) = \frac{i_{/\!/}(t) - i_{\perp}(t)}{i_{/\!/}(t) + 2i_{\perp}(t)} = \sum_j \beta_j \exp(-t/\phi_j) \quad (3)$$

where $i_{/\!/}(t)$ and $i_{\perp}(t)$ are, respectively, the parallel and perpendicular components of the fluorescence, τ is the fluorescent lifetime, and ϕ is the rotational correlation time. In fluorescence spectroscopy applied to biological systems, multiexponential decay is frequently encountered. Heterogeneity can arise from the same fluorophore, but localized in different environments, which affect the fluorescence decay rate differently. Alternatively, the nonexponential fluorescence decay can also be an intrinsic property of the chromophore itself, e.g., an excited state reaction. Multiexponential anisotropy decay can be caused by independent motion of the fluorescent probe superimposed on the slower motion of the macromolecular system into which the probe is incorporated.

The quantities that are obtained experimentally are $I_{/\!/}(t)$ and $I_{\perp}(t)$. These are convolutions of $i_{/\!/}(t)$ and $i_{\perp}(t)$ with the impulse response profile of the instrument $P(t)$. From $I_{/\!/}(t)$ and $I_{\perp}(t)$, the experimental fluorescence $S(t)$ can be calculated.

$$S(t) = I_{/\!/}(t) + 2I_{\perp}(t). \quad (4)$$

As stated above, the impulse response profile can be most accurately measured via the single-exponential fluorescence decay of the reference compound $S_r(t)$ according to the following convolution product:

$$S_r(t) = P(t) * \exp(-t/\tau_r). \quad (5)$$

Several methods exist to determine the decay parameters α_i and τ_i from $S(t)$ and $S_r(t)$ [14], [16], but the most popular among these is a nonlinear least squares fit of $S(t)$ according to the following relationship:

$$S(t) = s(0)\, S_r(t) + S_r(t) * X(t), \quad (6)$$

in which

$$X(t) = \sum_i \alpha_i \left(\frac{1}{\tau_r} - \frac{1}{\tau_i}\right) \exp(-t/\tau_i). \quad (7)$$

In this procedure, the weighted sum of squared residuals (WSSR) is minimized.

$$\text{WSSR} = \sum_{k=1}^{n} w_k [S(t_k) - S_c(t_k)]^2. \quad (8)$$

$S_c(t)$ is the calculated fit of $S(t)$, w_k is the weighting factor of data point $S(t_k)$, and n is the total number of data points.

Since the noise for single-photon counting data obeys Poisson statistics, the weighting factors, which equal the inverse of the variance of the data points, can easily be calculated from the variances of $I_{/\!/}(t)$ and $I_{\perp}(t)$ [19]–[21]. Sometimes a background of unwanted emission from impurities is present in the experimental data. When this background fluorescence cannot be neglected, which is often the case with biological samples, a recording of the background is subtracted, and the contribution to the noise in the fitted data points is taken into account.

Minimization of the WSSR can be performed with τ_r fixed, if an accurate value is known for it, or with τ_r as an extra iteration variable. A good method to obtain accurate values for the reference lifetime is to take two compounds, which decay single exponentially with lifetimes, which are not too close and have the two decays fitted simultaneously, with both lifetimes variable. A severe limitation of the reference method is that in the case where one of the τ values equals τ_r, this component will not be found in the analysis because of elimination of the term $(1/\tau_r - 1/\tau_i)$ in (7).

Determination of the anisotropy parameters β and ϕ can be done in several ways (see [22] for a survey). The method we use is a global analysis of $I_{/\!/}(t)$ and $I_{\perp}(t)$. When the expressions for $I_{/\!/}(t)$ and $I_{\perp}(t)$ are known, these quantities can be fitted simultaneously with one set of parameters. The basic expressions are [23]:

$$I_{/\!/}(t) = P(t) * i_{/\!/}(t) = P(t) * \{1/3\, s(t) + 2/3\, s(t)\, r(t)\} \quad (9a)$$

$$I_{\perp}(t) = P(t) * i_{\perp}(t) = P(t) * \{1/3\, s(t) - 1/3\, s(t)\, r(t)\} \quad (9b)$$

with $P(t)$ being the impulse response profile (see above) and $s(t)$ and $r(t)$ given in (2) and (3).

When a reference compound is used, the expressions $I_{/\!/}(t)$ and $I_{\perp}(t)$ are obtained by substitution of (2) and (3) into (9a) and (9b) and by the Laplace transform and inverse transform of the resulting expressions, giving

$$I_{/\!/}(t) = i_{/\!/}(0)\, S_r(t) + 1/3\, S_r(t) * X(t) + 2/3\, S_r(t) * Y(t) \quad (10a)$$

$$I_{\perp}(t) = i_{\perp}(0)\, S_r(t) + 1/3\, S_r(t) * X(t) - 1/3\, S_r(t) * Y(t) \quad (10b)$$

with

$$Y(t) = \sum_i \sum_j \left\{ \alpha_i \beta_j \left(\frac{1}{\tau_r} - \frac{1}{\tau_i} - \frac{1}{\phi_j}\right) \exp\left(-\frac{t}{\tau_i} - \frac{t}{\phi_j}\right)\right\}. \quad (11)$$

In the derivation of (10), it is assumed that when $s(t)$ and $r(t)$ are multiple exponential, all the cross terms for the different lifetimes τ_i and correlation times ϕ_j must be

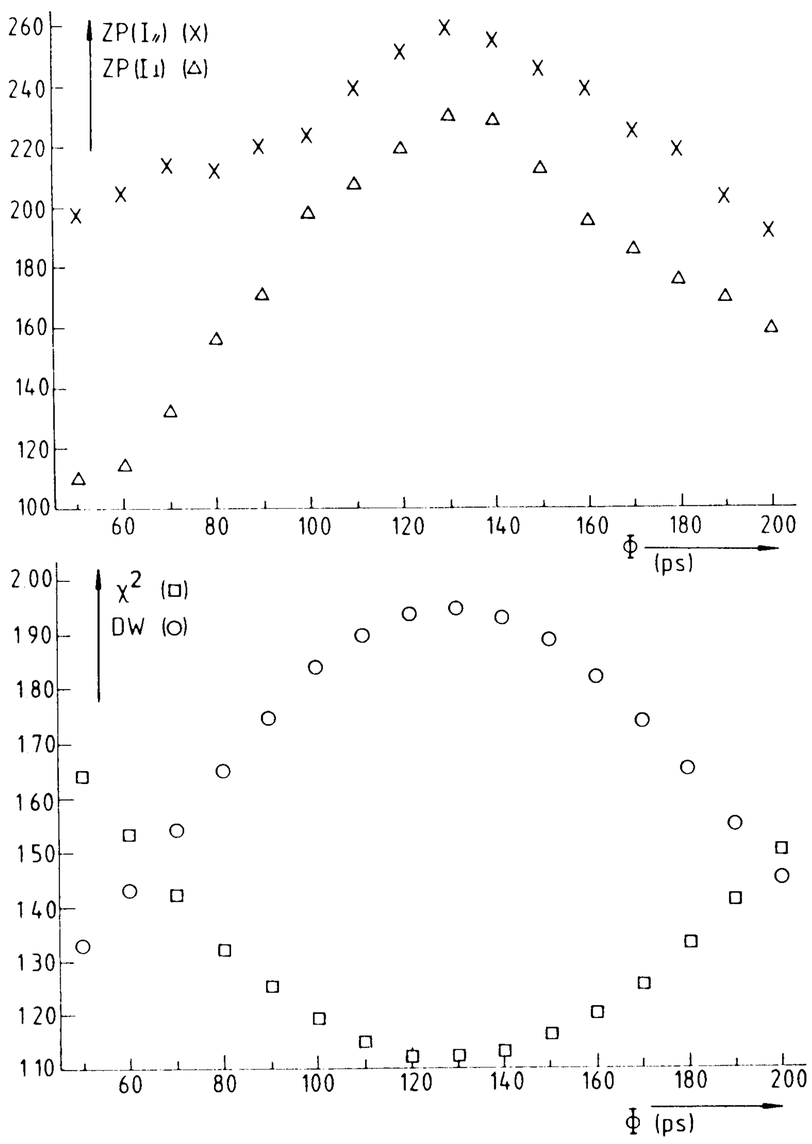

Fig. 2. Curves of χ^2, DW, ZP($I_{/\!/}$), and ZP($I_\perp$) versus rotational correlation time ϕ for the experiment detailed in Fig. 4(b).

accounted for. Physically, this means that every lifetime is coupled with every rotation. For instance, in the case of a mixture of two fluorescence compounds, each with a single lifetime and correlation time, these lifetimes must be associated with only one of the correlation times. Hence, the model has to be adapted, and some of the cross terms have to be omitted.

Using deconvolution procedures, decay times much shorter than the width of the temporal response function of the setup can be recovered. The time resolution is also dependent on the accuracy of the data (i.e., dependent on the number of counts) and the temporal stability of succeeding measurements. When the decay times become much shorter than the temporal response width, the accuracy of the determinations decreases. For instance, with a temporal response function of 500 ps FWHM, fluorescence decay times of 40 ps could be measured with an accuracy of better than 10 percent, including reproducibility of different experiments. We have used Rose Bengal in water as a reference compound on many different days of experiments and measured the fluorescence lifetime to be 66 $\pm$ 7 ps at 25°C (35 observations), and Rose Bengal in methanol was measured to be 530 $\pm$ 5 ps at 19°C.

Similar effects appear when analyzing the data of fluorescence anisotropy measurements. In that case, another important parameter is the initial anisotropy β at $t = 0$. In Fig. 2, graphs are presented of χ^2, DW, ZP($I_{/\!/}$), and ZP($I_\perp$) to illustrate the quality of the fit in the case of anisotropy measurements, with data from Fig. 4(b). β was fixed at 0.38, and χ^2, DW, ZP($I_{/\!/}$), and ZP($I_\perp$) were calculated for ϕ varying from 50 to 200 ps in 10 ps increments. It can be seen that there is a clear optimum for all parameters at ϕ about 130 ps. In the normal fit procedure, the iteration process optimizes for minimum χ^2 (8). Finally, DW, ZP($I_{/\!/}$), and ZP($I_\perp$) are calculated.

Applications

Four completely different examples will be presented to delineate the different approaches. We will first show that vitamin B_2 (riboflavin) can be easily detected in very low concentrations. In principle, by selective excitation and detection, it must be possible to observe this compound by virtue of its high quantum yield and single characteristic lifetime under *in vivo*-like conditions, e.g., intracellularly or in blood. The second example will deal with the observation of glutathione reductase, which is a flavin containing enzyme present in human erythrocytes. The flavin prosthetic group is flavin adenine dinucleotide (FAD), which is biosynthesized from riboflavin. Then a conformational study on an almost classic enzyme, alcohol dehydrogenase from horse liver, will be presented. Finally, we will show that information can be obtained from fluorescent lipids specifically inserted into natural membranes isolated from skeletal muscle.

The structural formulas of the chromophoric groups have been collected in Fig. 3.

The first two examples made use of the output of the argon ion laser as a source of excitation. In the latter two examples, a frequency-doubled synchronously pumped CW dye laser excited the samples.

Riboflavin

In mammalian systems, riboflavin or vitamin B_2 must be provided in the diet since it is, in contrast to bacteria, not synthesized. Riboflavin is the precursor metabolite in the biosynthesis of flavins, which are indispensable cofactors in all organisms. Riboflavin in neutral aqueous solution has a characteristic yellow color and gives rise to strong green fluorescence upon excitation with blue or UV light [24], [25].

The fluorescence decay is exponential, as illustrated in Fig. 4(a), leading to a single lifetime of 4.72 ns. The concentration used in this example amounted to 100 nM. A 100-fold lower concentration could easily be employed with retrieval of the same single lifetime. In this experiment, with excitation at 457.9 nm and detection at 531 nm, use was made of erythrosin B in water as a reference compound. Since the fluorescence lifetimes of riboflavin and erythrosin B are far apart, the lifetimes were fitted simultaneously, resulting in a value of 60 ps for the erythrosin fluorescence lifetime.

Riboflavin is a good example to set out the limits of the instrument for measurements of rotational correlation times, which are comparable to the actual laser pulsewidth (100 ps). The analysis of the experiment is shown in Fig. 4(b). It can be clearly seen in Fig. 4(b) that the anisotropy is created and decays within the fluorescence response curve of erythrosin B. Because the correlation time is shorter than the measured pulsewidth (500 ps), the anisotropy decay is distorted, and deconvolution is required to recover the correlation time of 128 ps at 20°C.

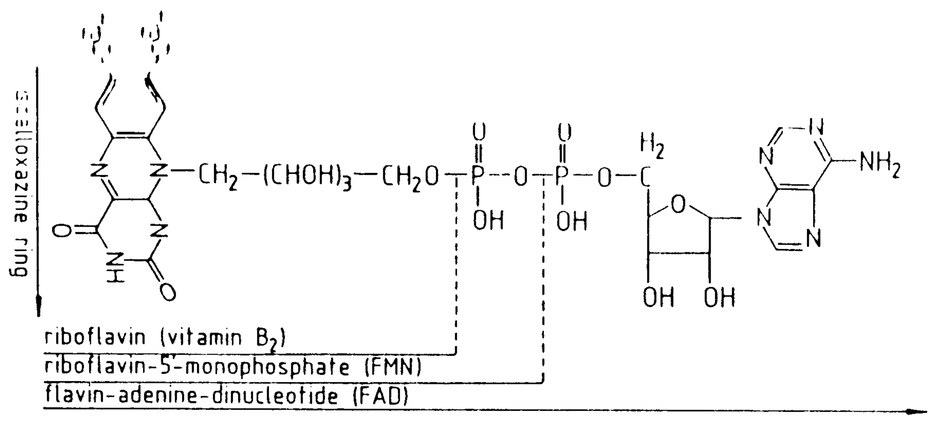

(a)

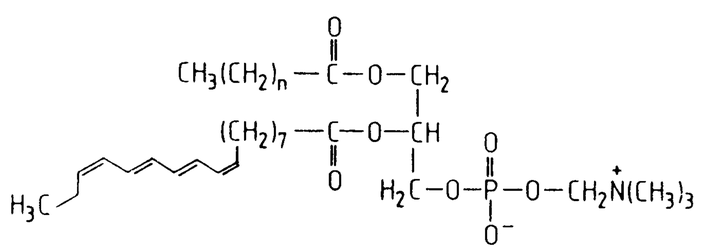

(b)

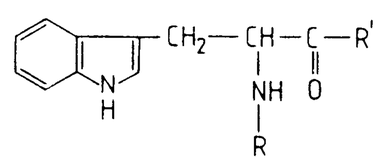

(c)

Fig. 3. Structural formulas of the chromophoric groups. (a) Flavins. (b) 1-acyl-2-*cis*-parinaroyl-*sn*-glycero-3-phosphocholine. (c) Tryptophan.

The rotational correlation time is slightly longer than that of the closely related lumazine molecule (83 ps) [9] or lumiflavin (60 ps) [26], but this is expected since the molecular volume of riboflavin is larger than that of the other two compounds. Short correlation times from less distorted anisotropy decay curves can be measured with faster detectors [27]. At the moment, a microchannel plate photomultiplier [5] is incorporated in the setup, and a decreased width of the instrumental response with a factor of 3 is observed.

Glutathione Reductase

Glutathione reductase (molecular weight 100 000) catalyzes the reduction of oxidized glutathione by nicotinamide adenine dinucleotide phosphate (NADPH, reduced form). Reduced glutathione has an important function in red blood cells, to maintain cysteine in blood proteins and the iron in the heme of hemoglobin in the reduced state. Moreover, it plays a role in detoxification of peroxides. The enzyme glucose-6-phosphate dehydrogenase is responsible for NADPH production. Deficiency of the latter enzyme may, in some cases, lead to hemolytic anemia induced by antimalarial drugs.

The fluorescence decay upon excitation with the 457.9 nm line of the argon ion laser is extremely complex since a model of a sum of four exponential terms had to be used to obtain an optimum fit. It is difficult to provide a good physical description of this multiexponential decay. The short fluorescence lifetime component has by far the largest amplitude. The shortening of the lifetime from, for example, 4.72 ns as observed in riboflavin (see above) to 0.05 ns can probably be ascribed to quenching of the flavin fluorescence by sulfur atoms. There is also a characteristic long fluorescence lifetime component of 5.5 ns, which is exceptional for flavoproteins.

From the three-dimensional structure of the protein [28], it is known that a cysteine residue is in the close

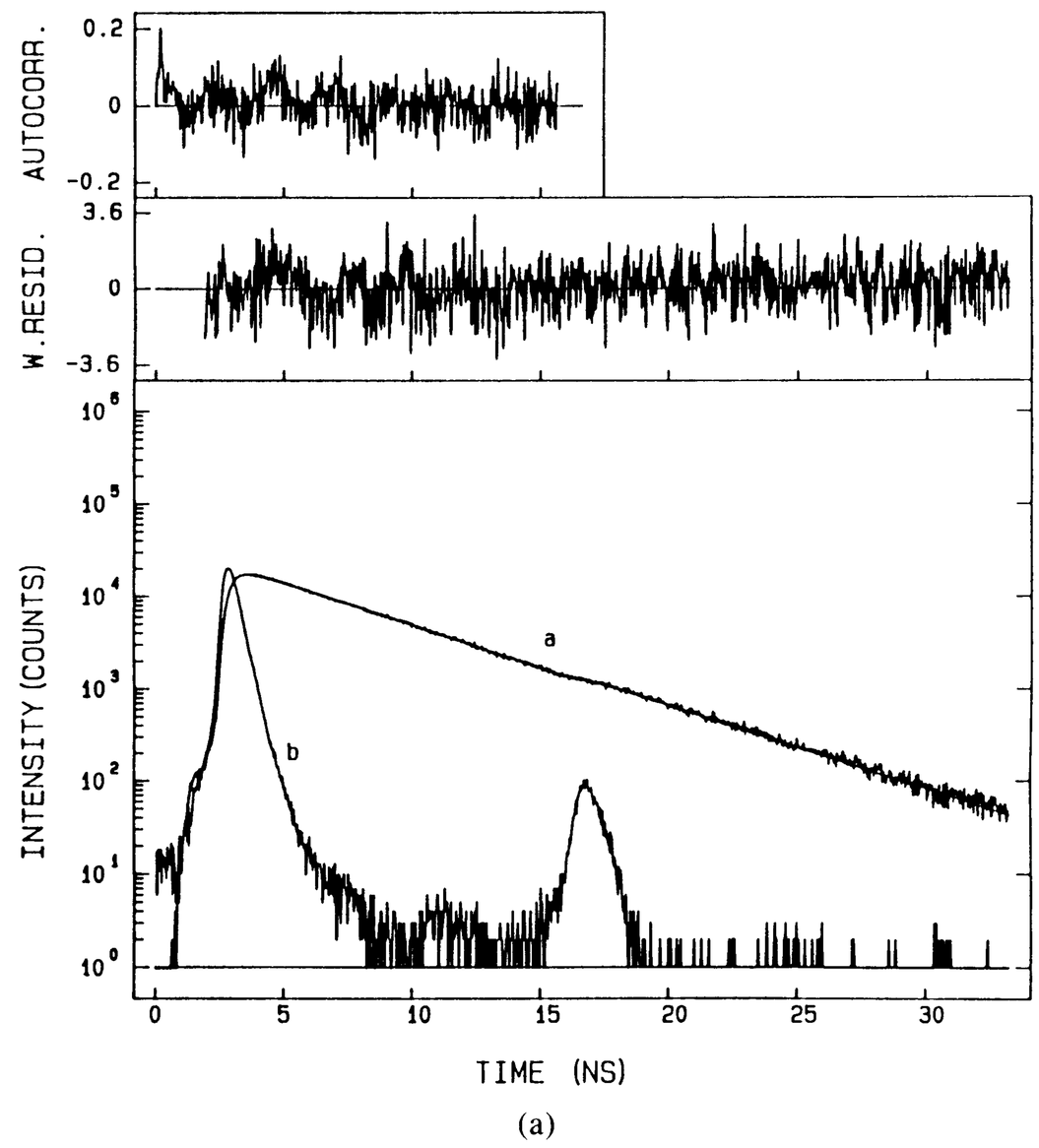

(a)

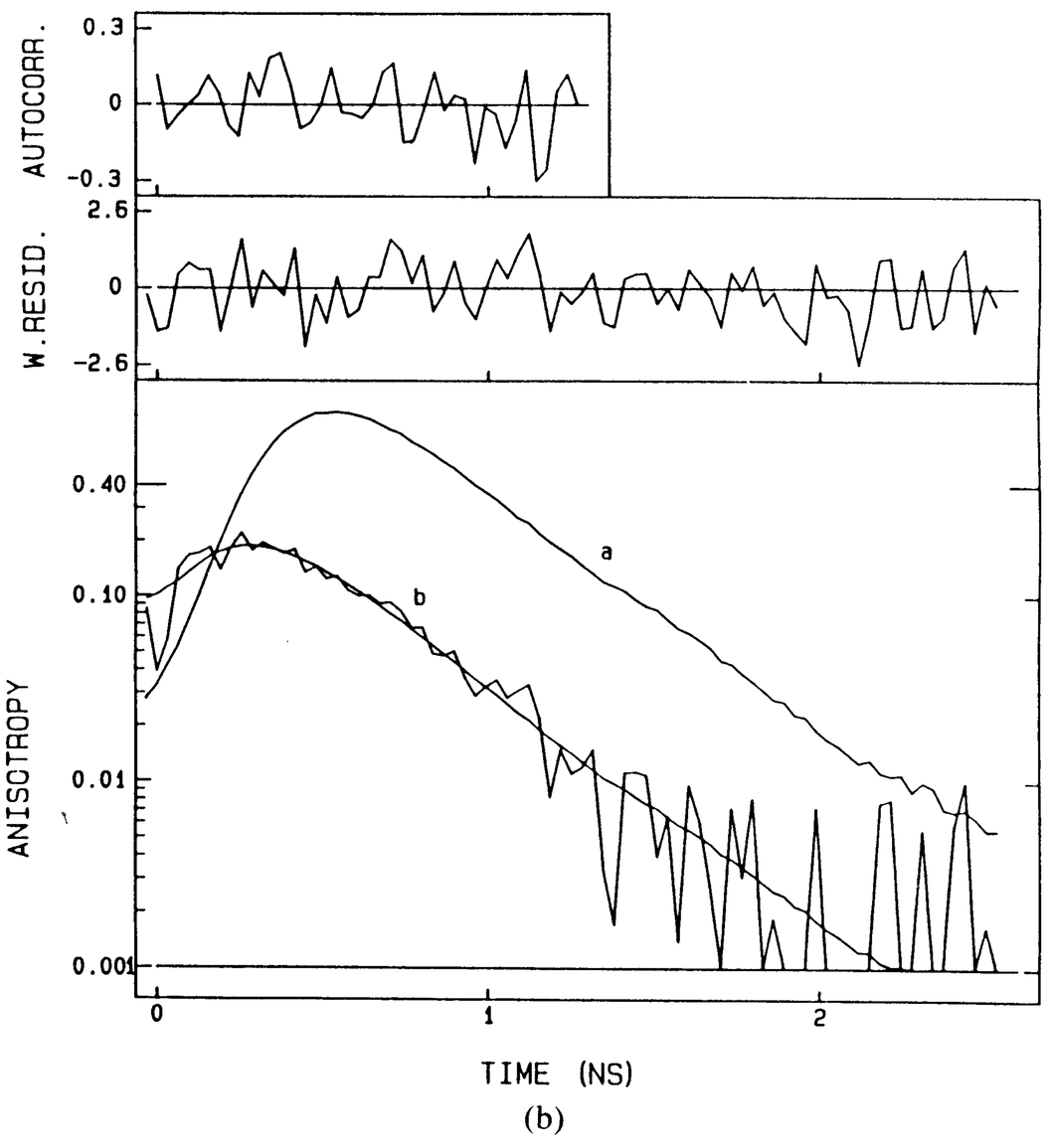

(b)

Fig. 4. (a) Fluorescence decay analysis of riboflavin (0.1 μM) in water pH 7.0 at 20°C with erythrosin B (10 μM) in water as reference compound. Wavelengths of excitation and emission were 457.9 and 531 nm, respectively. Shown are the fluorescence response curves of erythrosin B (curve b) and riboflavin (curve a) and the calculated riboflavin fluorescence with a lifetime of 4.715 $\pm$ 0.004 ns. The quality of the fit is indicated by the weighted residuals and autocorrelation function on top of the curves. χ^2 = 1.16, the Durbin–Watson parameter DW = 1.91, and the number of zero passages in the autocorrelation function ZP = 228 (1024 channels; time equivalence per channel was 0.032467 ns). The reference lifetime was fitted to 60 $\pm$ 1 ps. (b) Anisotropy decay analysis of riboflavin. Analysis was carried out over the whole decay curve of parallel and perpendicular components (1024 channels each). Shown is a replot over a limited time range of the fitted and experimental anisotropy (curve b). The correlation time amounted to 128 $\pm$ 3 ps; the initial anisotropy was fixed at 0.38. The fluorescence response curve (curve a) of erythrosin B is shown to illustrate the rise and decay of the anisotropy. χ^2 = 1.12, DW = 1.95, ZP($I_{/\!/}$) = 241, and ZP($I_{\perp}$) = 259.

vicinity of the flavin. Sulfur atoms are very efficient quenchers of flavin fluorescence [29]. Fluorescence quenching can be caused by a diffusion-controlled collision mechanism, leading to a shortening of the fluorescence lifetime. In a protein, on the other hand, the quenching of the fluorescence is caused by amino acid residues within the protein, and unlimited diffusion is impossible because of the constraints imposed by the polypeptide chain. Restricted diffusion may in part be responsible for the nonexponential decay pattern. The model of four exponential terms must be considered as a purely mathematical description.

Detection of glutathione reductase via its complex, but characteristic, fluorescence decay may provide diagnostic information. First, one can tune excitation and emission in such a way that flavoproteins can be selectively excited. β-carotene is one of the few other natural chromophores absorbing blue–green light from the visible spectrum, but this compound is characterized by very short-lived emission. Second, one can gate the observation window to relatively long times after the excitation pulse so that long-lived fluorescence of glutathione reductase can be selected. Human hereditary hemolytic anemia may result from a deficiency of several enzymes, including glutathione reductase.

If we assume homogeneous rotation, i.e., all fluorescence lifetime components are associated with the same rotational correlation time, the anisotropy decay gives rise to a surprisingly simple pattern (Fig. 5). The anisotropy decay is exponential, leading to a correlation time of 3.6 ns, which is too short to account for the rotation of the whole protein. The latter correlation time can be calculated to be 38 ns by an empirical formula relating correlation time to the molecular weight of a hydrated spherical protein. The correlation time of 3.6 ns suggests that a segmental motion of the protein is the predominant type of rotational dynamics of the protein.

Liver Alcohol Dehydrogenase (LADH)

LADH is one of the best-characterized proteins [30]. The enzyme catalyzes the NAD^+-assisted oxidation of alcohol. The enzyme consists of two identical subunits (the subunit molecular weight is 40 000). Each subunit contains two tryptophan residues, one of which is located near the protein surface, while the other is buried in the hydrophobic region near the subunit interface. Both tryptophan residues are associated with two different fluorescence lifetimes [31].

The anisotropy decay of the free enzyme [Fig. 6(a)] is exponential, and the rotational correlation time reflects the overall protein motion. The formation of a stable ternary complex between the enzyme, NADH, and an inhibitor of the enzyme (to prevent substrate turnover) resulted in different excited-state parameters. Besides the two lifetimes, which are the same as in the free protein, a major third component is found. This component originates from singlet–singlet energy transfer from tryptophan to NADH, leading to a more rapid fluorescence decay.

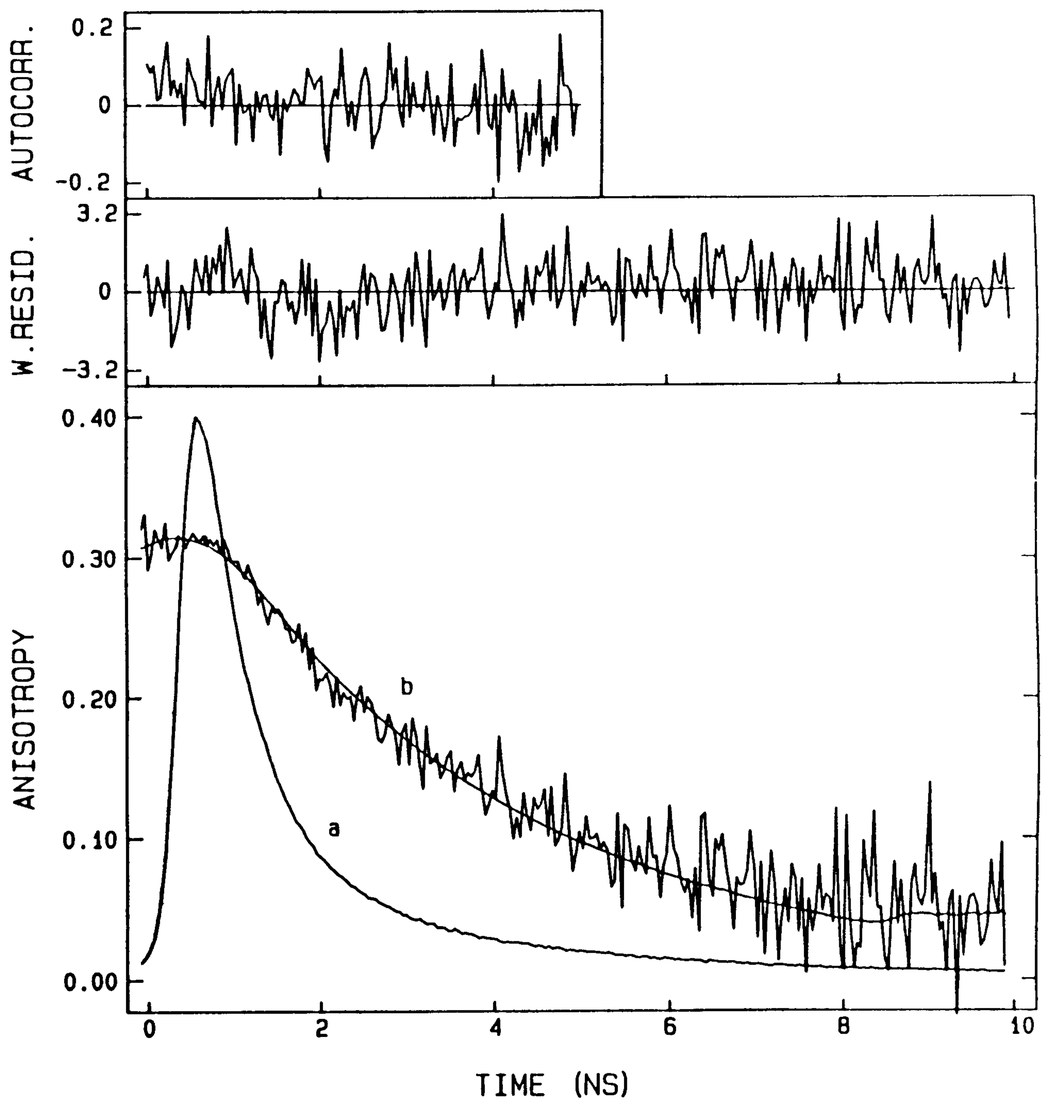

Fig. 5. Fluorescence anisotropy decay (curve b) of FAD in glutathione reductase from human erythrocytes at 20°C. Wavelengths of excitation and emission were 457.9 and 531 nm, respectively. Time equivalence per channel was 0.040053 ns. The fluorescence response curve (a) is shown in the same figure. See Fig. 1 for details of the analysis. The correlation time $\phi = 3.55 \pm 0.05$ ns, and the initial anisotropy is 0.322 $\pm$ 0.001. Fitting criteria: $\chi^2 = 1.74$, DW = 1.74, ZP($I_{/\!/}$) = 231, and ZP($I_\perp$) = 251.

The anisotropy decay [Fig. 6(b)] also changes upon formation of the ternary complex, which is an indication that the protein conformation changes upon binding of cofactor and inhibitor. A sum of two exponentials is needed to describe the decay satisfactorily in this case. The fast component, which is not present in the anisotropy decay of the free enzyme, has only very little contribution. It is so short that it can only be accounted for by an intramolecular segmental motion. The long rotational correlation time, which represents the overall protein motion, is about 10 percent shorter than in the case of the free enzyme. Apparently, there is some contraction of the protein matrix when the ternary complex is formed.

Fluorescent Membrane Probes

Another example of fluorescence anisotropy decay consists of the use of a long linear polyene of length similar to that of the fatty acid chain of most natural lipids [32]. These long unsaturated fatty acids occur in nature, and they are, upon incorporation into a lipid, very attractive fluorescent lipid probes because of their minimal perturbation. The quite strong fluorescence is in the violet-blue region of the spectrum and is far away from the absorption maxima in the 300–340 nm range. The large Stokes shift of the fluorescence is advantageous since scattering problems with natural membranes can be minimized. Natural membranes were labeled by incubating membrane preparations with a phospholipid transfer protein that specifically binds phosphatidylcholine lipid molecules [33]. In

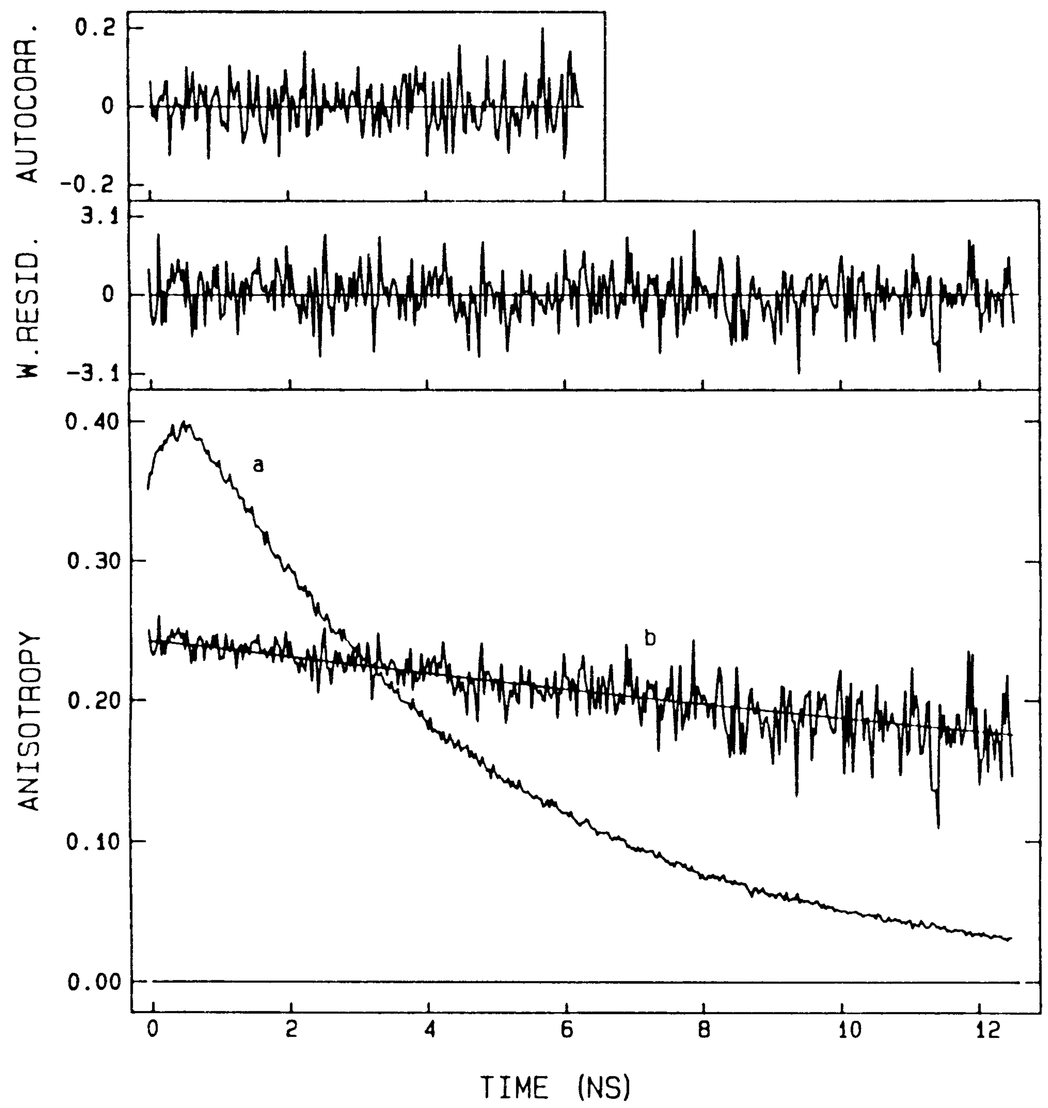

(a)

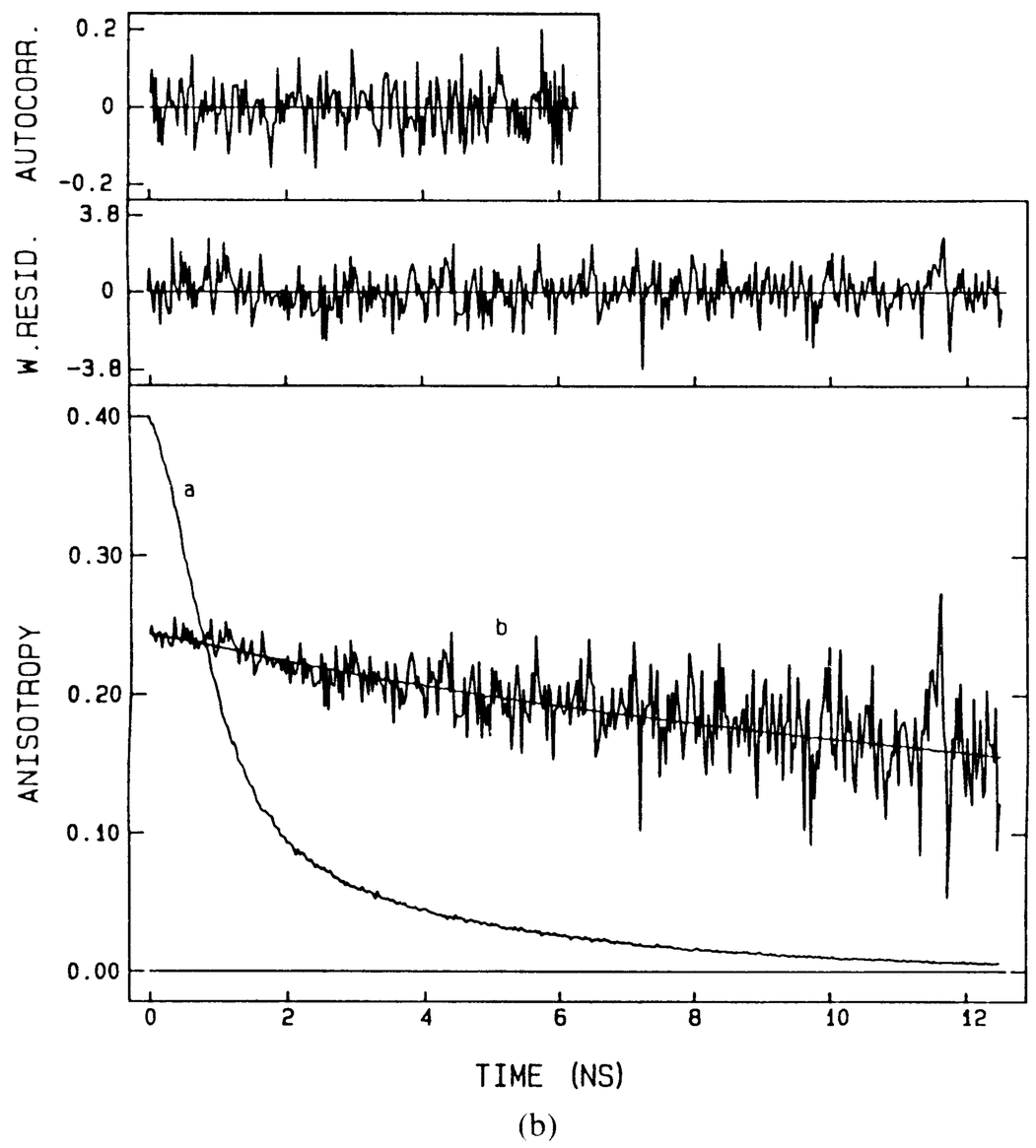

(b)

Fig. 6. (a) Fluorescence (curve a) and anisotropy (curve b) decays of horse liver alcohol dehydrogenase at 20°C. (b) The ternary complex of this enzyme with the inhibitor isobutyramide and the cofactor NADH at 20°C. Excitation and emission wavelengths were 300 and 337 nm, respectively. Time equivalence per channel was 0.031413 ns. In the fluorescence decay of the ternary complex, the fast component, caused by tryptophan-to-NADH energy transfer, is clearly present. The anisotropy parameters are as follows. (a) $\beta = 0.224 \pm 0.001$, $\phi = 36.2 \pm 1.0$ ns with $\chi^2 = 1.02$, DW = 1.98, ZP($I_{/\!/}$) = 220, and ZP($I_{\perp}$) = 257. (b) $\beta_1 = 0.02 \pm 0.01$, $\phi_1 = 2.6 \pm 0.4$, $\beta_2 = 0.20 \pm 0.01$, $\phi_2 = 33.1 \pm 1.2$ ns with $\chi^2 = 1.05$, DW = 1.90, ZP($I_{/\!/}$) = 238, and $ZP(I_{\perp})$ = 213.

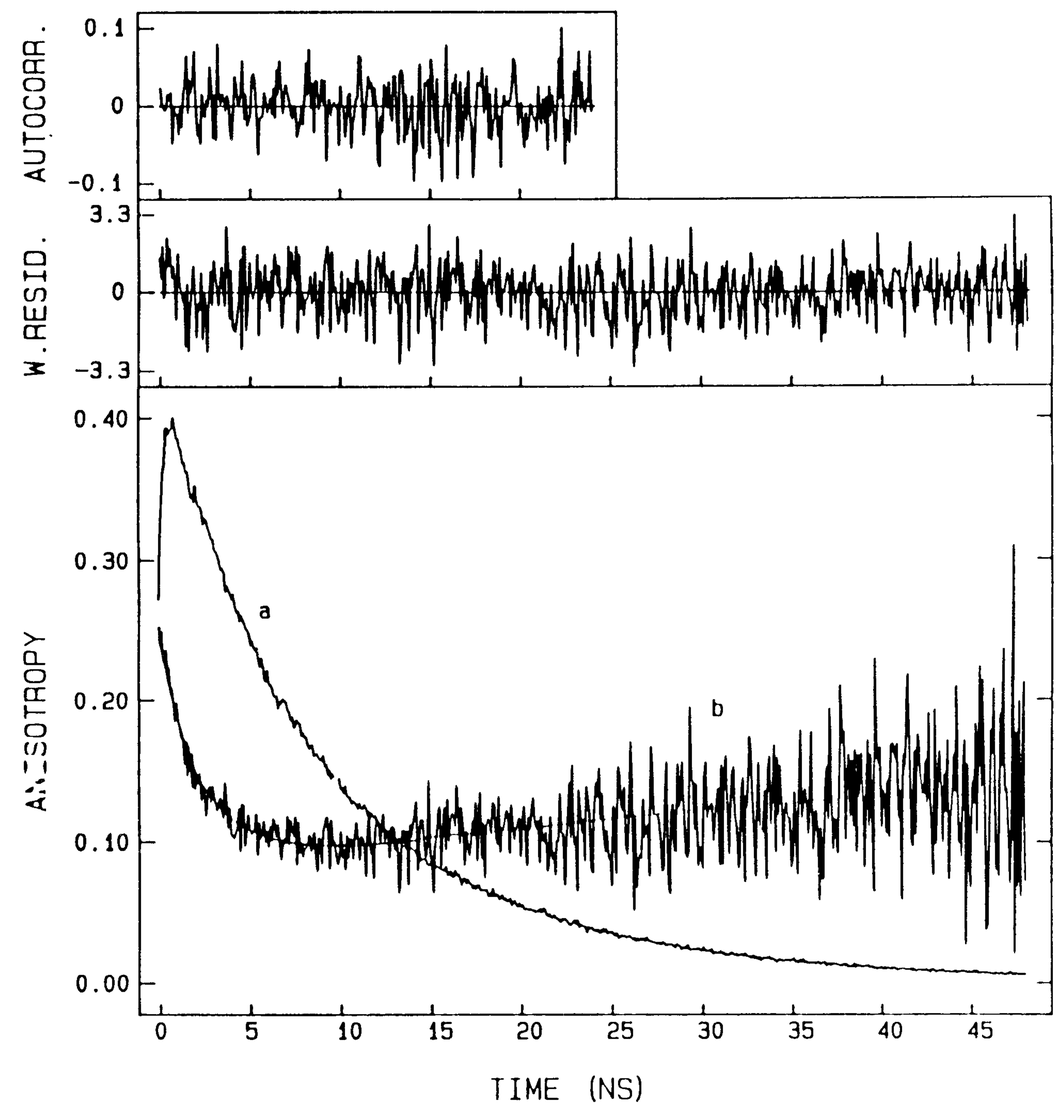

Fig. 7. Fluorescence anisotropy decay of 2-parinaroyl-phosphatidylcholine in rat skeletal muscle sarcolemmal membranes at 20°C. The excitation wavelength was 304 nm, and the fluorescence was selected through a K45 Balzers bandpass filter. Time equivalence per channel was 0.086956 ns. The noisy curve (curve b) indicates the experimental data, while the fitted decay function is represented by the smooth line. The fluorescence anisotropy clearly does not decay to a constant value, but rises again after having reached a minimum. The fluorescence response curve (curve a) is presented in the same figure. The figure shows the results obtained with a model in which two fluorescence lifetimes were coupled to two separate restricted rotational motions. The analysis for the population connected with the shorter lifetime ($\tau = 7.1$ ns) resulted in a correlation time of 1.2 ns and a residual anisotropy $r(\infty)$ of 0.035. The longer fluorescence lifetime ($\tau = 16.0$ ns) corresponded with a correlation time of 3.1 ns and $r(\infty) = 0.140$. The fitting parameters were $\chi^2 = 1.38$, DW = 1.76, ZP($I_{/\!/}$) = 181, and ZP($I_{\perp}$) = 208.

this way, parinaroyl–phosphatidylcholine was incorporated in membranes isolated from rat skeletal muscle.

Information can be obtained on acyl chain order and dynamics. The ordering of the parinaric acid residues is manifested by a so-called residual time-independent anisotropy. The dynamics is characterized by a rapid initial anisotropy decay with a certain correlation time to the constant residual anisotropy.

The experiments on natural membranes gave the unexpected result that the fluorescence anisotropy decays initially, but after reaching a minimum, the anisotropy increases in time (Fig. 7). The latter phenomenon can be explained by assuming a distribution of probe molecules over different membrane regions. A limited population analysis could be performed by linking the short fluorescence lifetime component of the biexponential decay to one class with a particular residual anisotropy and correlation time and the longer fluorescence lifetime to another class with different residual anisotropy and correlation time (see caption of Fig. 7). Details of the analysis have recently been provided [34].

Time-resolved fluorescence anisotropy patterns as shown in Fig. 7 are the rule rather than the exception when

lipid probes are inserted into natural membranes. Biological membranes are heterogeneous systems composed of a variety of lipid molecules and intrinsic membrane proteins. The fluorescence probes are expected to be partitioned among different membrane regions of different fluidity and are therefore characterized by different fluorescence decay and anisotropy decay parameters.

Conclusion

Four different examples of time-resolved polarized fluorescence spectroscopy have been presented in this study in order to illustrate the versatility of the possible applications.

The first two examples dealt with the flavin chromophoric group, free in solution and, as most frequently encountered in biological systems, bound as a prosthetic group in an enzyme or protein.

The third example described the use of time-resolved fluorescence in the detection of conformational changes in alcohol dehydrogenase from liver, induced by the binding of coenzyme and inhibitor, and the occurrence of energy transfer from tryptophan to bound NADH within a single protein molecule.

The last example described experiments with a fluorescent lipid probe inserted into natural membranes. The characteristic anisotropy pattern changed when either other specific lipid probes or other membranes were used [35]. The other membranes were, among others, sarcolemmal membranes from denervated skeletal muscle. The latter membranes are richer in certain membrane proteins, like acetylcholine receptor, than the normal sarcolemmal membranes. The changing anisotropy patterns in both membranes may then provide a means to distinguish between these membranes.

It is shown that time-resolved polarized fluorescence spectroscopy is a powerful technique in biological and medical research, supplying diagnostic information in a few cases. The experiments were conducted in purified biological samples, which is essential for an appropriate interpretation of the anisotropy results. For *in situ* measurements in cells or organelles, a fluorescence microscope can be incorporated in the setup. Time-correlated single-photon counting with fluorescence microscopes has recently been described [36]–[38].

Acknowledgment

The authors thank Dr. A. de Kok for making the data on glutathione reductase available to them. Dr. P. van Paridon and Prof. K. Wirtz are acknowledged for providing the experimental data on fluorescent labeled sarcolemmal membranes.

References

[1] R. E. Dale, "Membrane structure and dynamics by fluorescence probe depolarization kinetics," in *Time-Resolved Fluorescence Spectroscopy in Biochemistry and Biology*, R. B. Cundall and R. E. Dale, Eds. (NATO ASI Series, Vol. 69). New York: Plenum, 1983, pp. 555–605.

[2] J. R. Lakowicz, *Principles of Fluorescence Spectroscopy*. New York: Plenum, 1983.

[3] S. R. Meech, C. D. Stubbs, and D. Phillips, "The application of fluorescence decay measurements in studies of biological systems," *IEEE J. Quantum Electron.*, vol. QE-20, pp. 1343–1352, 1984.

[4] N. E. Geacintov, D. Husiak, T. Kolubayev, J. Breton, A. J. Campillo, S. L. Shapiro, K. R. Winn, and P. K. Woodbridge, "Exciton annihilation versus excited state absorption and stimulated emission effects in laser studies of fluorescence quenching of chlorophyll *in vitro* and *in vivo*," *Chem. Phys. Lett.*, vol. 66, pp. 154–158, 1979.

[5] D. Bebelaar, "Time response of various types of photomultipliers and its wavelength dependence in time-correlated single photon counting with an ultimate resolution of 47 ps FWHM," *Rev. Sci. Instrument.*, vol. 57, pp. 1116–1125, 1986.

[6] G. S. Beddard, T. Doust, S. R. Meech, and D. Phillips, "Synchronously pumped dye lasers in fluorescence decay measurements of molecular motion," *J. Photochem.*, vol. 17, pp. 427–433, 1981.

[7] S. Kobayashi, M. Yamashita, T. Sato, and S. Muramatsu, "A single photon sensitive synchroscan streak camera for room temperature picosecond emission dynamics of adenine and polyadenylic acid," *IEEE J. Quantum Electron.*, vol. QE-20, pp. 1383–1385, 1984.

[8] A. J. W. G. Visser and A. van Hoek, "The fluorescence decay of reduced nicotinamides in aqueous solution after excitation with a UV mode-locked Ar ion laser," *Photochem. Photobiol.*, vol. 33, pp. 35–40, 1981.

[9] A. J. W. G. Visser, T. Ykema, A. van Hoek, D. J. O'Kane, and J. Lee "Determination of rotational correlation times from deconvoluted fluorescence anisotropy decay curves. Demonstration with 6.7-dimethyl-8-ribityllumazine and lumazine protein from *Photobacterium leiognathi* as fluorescent indicators," *Biochem.*, vol. 24, pp. 1489–1496, 1985.

[10] J. Hala, G. F. W. Searle, T. J. Schaafsma, A. van Hoek, P. Pancoska, K. Blaha, and K. Vacek, "Picosecond laser spectroscopy and optically detected magnetic resonance on a model photosynthetic system," *Photochem. Photobiol.*, vol. 44, pp. 527–534, 1986.

[11] A. van Hoek, J. Vervoort, and A. J. W. G. Visser, "A subnanosecond resolving spectrofluorimeter for analysis of protein fluorescence kinetics," *J. Biochem. Biophys. Methods*, vol. 7, pp. 243–254, 1983.

[12] A. van Hoek and A. J. W. G. Visser, "Pulse selection system with electro-optic modulators applied to mode-locked CW lasers and time-resolved single photon counting," *Rev. Sci. Instrument.*, vol. 52, pp. 1199–1205, 1981.

[13] D. V. O'Connor and D. Phillips, *Time Correlated Single Photon Counting*. New York: Academic, 1984.

[14] D. V. O'Connor, W. R. Ware, and J. C. Andre, "Deconvolution of fluorescence decay curves," *J. Phys. Chem.*, vol. 83, pp. 1333–1343, 1979.

[15] A. van Hoek and A. J. W. G. Visser, "Artifact and distortion sources in time-correlated single photon counting," *Anal. Instrument.*, vol. 14, pp. 359–378, 1985.

[16] M. van den Zegel, N. Boens, D. Daems, and F. C. de Schryver, "Possibilities and limitations of the time-correlated single photon counting technique: A comparative study of correction methods for wavelength dependence of the instrumental response function," *Chem. Phys.*, vol. 101, pp. 311–335, 1986.

[17] R. A. Lampert, L. A. Chewter, D. Phillips, D. V. O'Connor, A. J. Roberts, and S. R. Meech, "Standards for nanosecond fluorescence decay time measurements," *Anal. Chem.*, vol. 55, pp. 69–73, 1983.

[18] K. Vos, A. van Hoek, and A. J. W. G. Visser, "Applications of a reference convolution method to tryptophan fluorescence in proteins. A refined description of rotational dynamics," *Eur. J. Biochem.*, vol. 165, pp. 55–63, 1987.

[19] P. R. Bevington, *Data Reduction and Error Analysis for the Physical Sciences*. New York: McGraw-Hill, 1969.

[20] Ph. Wahl, "Statistical accuracy of rotational correlation times determined by the photon counting pulse fluorimetry," *Chem. Phys.*, vol. 22, pp. 245–256, 1977.

[21] ——, "Analysis of fluorescence anisotropy decays by a least squares method," *Biophys. Chem.*, vol. 10, pp. 91–104, 1979.

[22] D. Phillips, R. C. Drake, D. V. O'Connor, and R. L. Christensen, "Time-correlated single-photon counting (TCSPC) using laser excitation," *Anal. Instrument.*, vol. 14, pp. 267–292, 1986.

[23] J.-E. Löfroth, "Deconvolution of single photon counting data with a reference method and global analysis," *Eur. Biophys. J.*, vol. 13, pp. 45–58, 1985.

[24] A. J. W. G. Visser and A. van Hoek, "The measurement of subnanosecond fluorescence decay of flavins using time-correlated photon

counting and a mode-locked Ar ion laser,'' *J. Biochem. Biophys. Methods*, vol. 1, pp. 195–208, 1979.
[25] A. J. W. G. Visser, J. S. Santema, and A. van Hoek, ''Spectroscopic and dynamic characterization of FMN in reversed micelles entrapped water pools,'' *Photochem. Photobiol.*, vol. 39, pp. 11–16, 1984.
[26] J. P. C. Bootsma, G. Challa, A. J. W. G. Visser, and F. Müller, ''Polymer-bound flavins: 5. Characterization by static and time resolved fluorescence techniques,'' *Polymer*, vol. 26, pp. 951–956, 1985.
[27] R. Rigler, F. Claesens, and O. Kristensen, ''Picosecond fluorescence spectroscopy in the analysis of structure and motion of biopolymers,'' *Anal. Instrument.*, vol. 14, pp. 525–546, 1985.
[28] R. Thieme, E. F. Pai, R. H. Schirmer, and G. E. Schultz, ''Three-dimensional structure of gluthathione reductase at 2 Å resolution,'' *J. Mol. Biol.*, vol. 152, pp. 763–782, 1981.
[29] M. C. Falk and D. B. McCormick, ''Synthetic flavinyl peptides related to the active site of mitochondrial monoamine oxidase. II Fluorescence properties,'' *Biochem.*, vol. 15, pp. 646–653, 1976.
[30] C. I. Brändén, H. Jörnvall, H. Eklund, and B. Furugren, ''Alcohol dehydrogenases,'' in *The Enzymes*, vol. 11, 3rd ed., P. D. Boyer, Ed. New York: Academic, 1975, pp. 103–190.
[31] J. B. A. Ross, C. J. Schmidt, and L. Brand, ''Time-resolved fluorescence of the two tryptophans in horse liver alcohol dehydrogenase,'' *Biochem.*, vol. 20, pp. 4369–4377, 1981.
[32] L. A. Sklar, B. S. Hudson, M. Petersen, and J. Diamond, ''Conjugated polyene fatty acids on fluorescent probes: Spectroscopic characterization,'' *Biochem.*, vol. 16, pp. 813–819, 1977.
[33] T. A. Berkhout, A. J. W. G. Visser, and K. W. A. Wirtz, ''Static and time-resolved studies of fluorescent phosphatidylcholine bound to the phosphatidylcholine transfer protein of bovine liver,'' *Biochem.*, vol. 23, pp. 1505–1513, 1984.
[34] A. J. W. G. Visser, A. van Hoek, and P. A. van Paridon, ''Time-resolved fluorescence depolarization studies of parinaroyl phosphatidylcholine in Triton X-100 micelles and rat skeletal muscle membranes,'' in *Membrane Receptors, Dynamics and Energetics* K. W. A. Wirtz, Ed. New York: Plenum, 1987, pp. 353–362.
[35] K. W. A. Wirtz, P. A. van Paridon, A. J. W. G. Visser, and B. de Kruijff, ''Structure and function of phosphoinositides in membranes and cells,'' in *Membrane Receptors, Dynamics and Energetics*, K. W. A. Wirtz, Ed. New York: Plenum, 1987, pp. 341–352.
[36] M. A. Rodgers and P. A. Firey, ''Instrumentation of fluorescence microscopy with picosecond time resolution,'' *Photochem. Photobiol*, vol. 42, pp. 613–616, 1985.
[37] H. Schneckenburger, ''Time-resolved microfluorescence in biomedical diagnosis,'' *Opt. Eng.*, vol. 24, pp. 1042–1044, 1985.
[38] T. Minami, M. Kawahigashi, Y. Sakai, K. Shimanoto, and S. Hirayama, ''Fluorescence lifetime measurements under a microscope by the time-correlated single-photon counting technique,'' *J. Luminescence*, vol. 35, pp. 247–253, 1986.

A. van Hoek, photograph and biography not available at the time of publication.

K. Vos, photograph and biography not available at the time of publication.

A. J. W. G. Visser, photograph and biography not available at the time of publication.